Biocybernetics and Biomedical Engineering 45 (2025) 476–484

Contents lists available at ScienceDirect

Biocybernetics and Biomedical Engineering

journal homepage: www.elsevier.com/locate/bbe

Research Paper

Movement and force dynamics in bimanual cooperative tasks in chronic stroke and healthy individuals

J. Podobnik *, M. Munih, M. Mihelj

University of Ljubljana, Faculty of Electrical Engineering, Tržaška c. 25, Ljubljana, SI-1000, Slovenia

ARTICLE INFO

Keywords:
Bimanual coordination
Haptic robot
Movement dynamics
Cooperative movements

ABSTRACT

Stroke rehabilitation often involves the use of haptic robots to improve motor control and bimanual coordination. This study examines how damping affects movement and force dynamics in bimanual tasks performed by healthy participants and participants with chronic stroke using a haptic robotic system equipped with force sensors for each hand. Participants completed tasks at three damping levels: 0 $\frac{\mathrm{N}}{\mathrm{m/s}}$ (no damping), 20 $\frac{\mathrm{N}}{\mathrm{m/s}}$ (low damping), and 40 $\frac{\mathrm{N}}{\mathrm{m/s}}$ (moderate damping). Key parameters for trajectory of movement, velocity, manipulation force, and internal force were analyzed to assess movement stability and control. The results revealed that damping 20 $\frac{\mathrm{N}}{\mathrm{m/s}}$ effectively stabilized movements in persons with stroke, reducing velocity deviations and making their performance more comparable to healthy participants, without introducing excessive resistance. In contrast, damping 40 $\frac{\mathrm{N}}{\mathrm{m/s}}$ acted as resistance training. Participants with stroke exhibited consistently higher internal forces than healthy participants, reflecting compensatory strategies and inefficient motor control. These findings demonstrate that low damping (20 $\frac{\mathrm{N}}{\mathrm{m/s}}$) offers an optimal balance between movement stabilization and resistance, highlighting its potential as a rehabilitation strategy, while moderate damping (40 $\frac{\mathrm{N}}{\mathrm{m/s}}$) may be reserved for resistance training.

1. Introduction

Stroke is a major cause of long-term disability, often impairing upper limb function and motor control [1]. Since many daily tasks depend on coordinated bimanual movements [2,3], restoring arm use is essential for functional independence. To address these impairments, rehabilitation strategies increasingly focus on restoring coordinated movements. Research by Rose [4] emphasized the potential of bimanual training to enhance motor recovery post-stroke, suggesting that coordinated bilateral movements could facilitate paretic limb performance by leveraging interlimb coupling effects, such as increased peak velocity during rapid aiming tasks. Recent meta-analyses confirm that bimanual training, especially when assisted by haptic robots, improves upper limb function in individuals with stroke, including those in chronic stages [5–8]. These interventions promote dexterity, grip strength, and functional gains, possibly through contralesional hemisphere involvement. Effective bimanual coordination requires both trajectory and force control [9], yet conventional assessments are often subjective, coarse, and lack real-time feedback–limiting their utility for adaptive rehabilitation [10].

Haptic robots address these limitations by offering precise, objective measurements of movement, force, and velocity while ensuring controlled, repeatable conditions [11–13]. Systematic reviews, including those summarized by Yang et al. [5], highlight that end-effector devices like the HapticMaster, are particularly effective for improving proximal arm function, such as reaching tasks, which are integral to bimanual cooperative protocol. Haptic interfaces enhance motor learning and interlimb coordination by providing real-time force feedback [4]. Adjustable difficulty and resistance levels allow standardized comparisons across individuals and sessions. Integration with virtual environments further enhances engagement and provides real-time feedback for movement adjustments.

Kanak et al. [7] state that bimanual movements can be classified by task goal, distinguishing between independent and common task goals. Within common task goal category, further distinction is made between parallel tasks, where interaction between arms is not necessary, and cooperative tasks, which require coordination between the limbs.

Resistance training, achieved through velocity-dependent damping in robotic devices, applies controlled resistance to the hemiparetic limb,

* Corresponding author.
E-mail address: janez.podobnik@fe.uni-lj.si (J. Podobnik).

https://doi.org/10.1016/j.bbe.2025.07.002
Received 10 March 2025; Received in revised form 2 July 2025; Accepted 7 July 2025
Available online 13 July 2025

improving motor control and strength [14–17]. Robotic devices achieve this through constant forces or velocity-dependent viscous resistance, where resistance increases with movement speed. The latter can be adjusted by modifying the damping coefficient.

While the benefits of damping in motor training are increasingly recognized, the selection of specific damping values remains largely empirical. Prior studies suggest that moderate values, typically in the range of (10–50 $\frac{\mathrm{N}}{\mathrm{m/s}}$), provide sufficient damping to stabilize movement without compromising voluntary control [12,18,19], supporting the minimal intervention principle, which posits that only task-relevant deviations require correction [20].

Evidence from clinical and preclinical studies shows that damping can improve performance: adaptive damping reduced hand oscillations in bimanual laparoscopic tasks [21], and spring-damper assistance improved tracking and interaction forces compared to undamped settings [22,23]. However, most prior work emphasizes stiffness, with the role of velocity-dependent damping remaining underexplored. Küçüktabak et al. [22] in his review concluded that additional study of the effect of velocity-dependent forces on task performance is warranted.

This study examines bimanual movement trajectories in persons with stroke using a specially designed bimanual haptic robot system. To address the limited understanding of velocity-dependent damping in bimanual training, we systematically varied damping levels (0 $\frac{\mathrm{N}}{\mathrm{m/s}}$, 20 $\frac{\mathrm{N}}{\mathrm{m/s}}$, and 40 $\frac{\mathrm{N}}{\mathrm{m/s}}$) to examine their effects on bimanual coordination in healthy and stroke participants. The low level (20 $\frac{\mathrm{N}}{\mathrm{m/s}}$) was selected to provide minimal stabilization without resistance, while the moderate level (40 $\frac{\mathrm{N}}{\mathrm{m/s}}$) introduced resistance without inducing fatigue. These values were chosen based on pilot testing and prior studies in haptic interaction and stroke rehabilitation [12,24]. Using a custom bimanual haptic robot equipped with independent force sensors for each hand, we analyzed how these damping levels influence movement trajectories and interaction forces during cooperative tasks requiring coordinated bilateral effort. Specifically, we investigated trajectory, velocity, manipulation forces (the sum of left and right forces that move the robot), and internal forces (the difference between left and right forces that do not contribute to movement). This approach enables a detailed evaluation of how damping influences movement stability, coordination strategies, and compensatory behaviors in bimanual motor control.

2. Methodology

2.1. Participants

Both healthy participants and participants with chronic stroke were included in the study. The study included 13 participants with chronic stroke (8 male, 5 female; aged 45–83 years, mean 57 ± 11) and 25 healthy participants (19 male, 6 female; aged 23–72 years, mean 36 ± 15). All participants were right-hand dominant. Among participants with chronic stroke, 8 had right arm paresis and 5 had left arm paresis, with post-stroke duration ranging from 5 to 27 years (mean 12 ± 9). This chronic phase (typically defined as >6 months post-stroke) suggests that motor recovery may have plateaued for these participants, potentially influencing task performance due to established compensatory strategies [25,26]. The study was approved by the Medical Ethics Committee of the Republic of Slovenia (80/03/15). All participants in the study signed a consent form on participation and use of data for scientific purposes.

2.2. Bimanual robotic measurement system

The experimental setup comprises a HapticMaster (MOOG FCS) robot with an added rotational degree of freedom and a custom instrumented handle for independent bilateral force measurements. The system, shown in Fig. 1, features three primary degrees of freedom plus the additional horizontal rotation to enable complex movements.

The handle system (Fig. 2a) incorporates dual JR3 50M31 6 DOF force/torque sensors to measure three-directional forces from each arm independently. These sensors provide force data during bilateral coordination. The local coordinate frame is shown in Fig. 2a. For participants with limited grip strength, an ergonomic brace was used to secure the impaired limb without compromising task performance or comfort (Fig. 2b).

Force sensors measure interaction forces, enabling admittance-controlled bimanual manipulation where the haptic robot responds to applied forces. This algorithm runs in the xPC Target real-time environment (The MathWorks Inc.) using MATLAB and Simulink. The haptic robot is velocity-controlled via a PID servo loop, with $\mathbf{v}_d$ as the reference input [27]. Reference velocity $\mathbf{v}_d$ is calculated by integrating

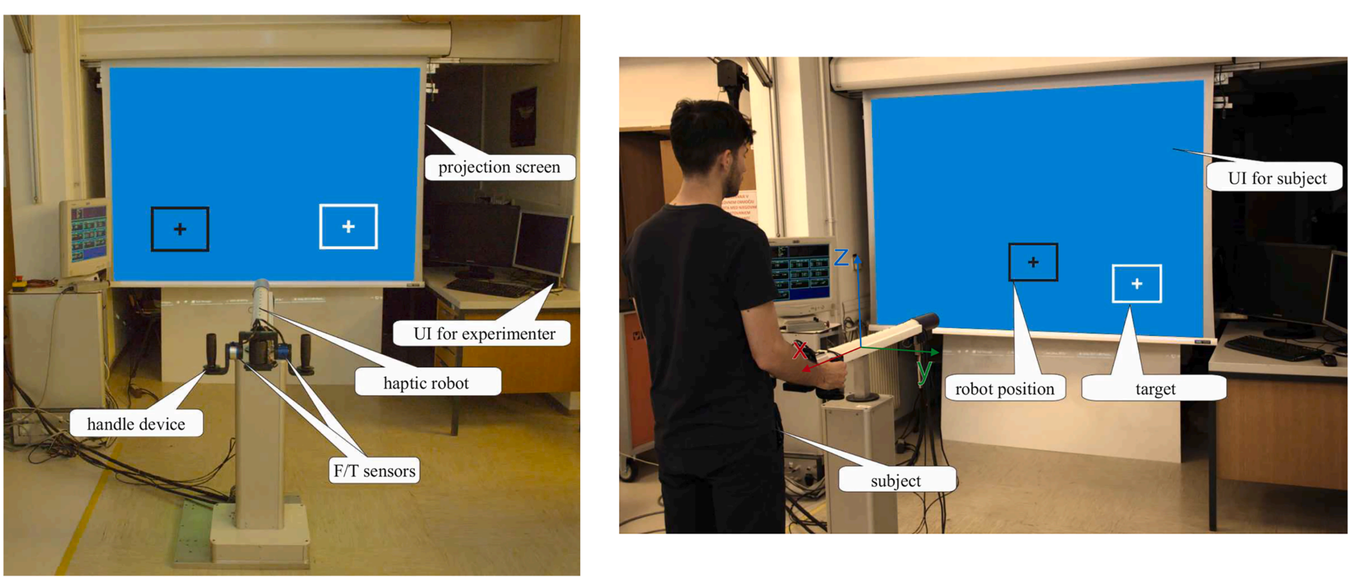

a b

Fig. 1. The figure depicts the experimental setup, featuring a HapticMaster haptic robot, a handle device with two F/T sensors for measuring hand forces, and a projection screen displaying targets and the robot's position marker (subfigure a). Subfigure (b) illustrates participants performing the task within the global coordinate frame, with movements in the YZ plane and rotations around the X-axis.

Fig. 2. The figure shows an instrumented handle system with two F/T sensors–one for each hand–and its local coordinate frame. Rotations occur about the X-axis (subfigure a). Subfigure (b) shows how participants place their hands on the instrumented handle with attached ergonomic brace (annotated with red border).

desired acceleration $\mathbf{a}_d$ which is calculated from forces. The following set of equations gives the control algorithm:

$$m \cdot \mathbf{a}_d = \mathbf{F}_L + \mathbf{F}_R - \mathbf{F}_D, \tag{1}$$

$$\mathbf{F}_D = B \cdot \mathbf{v}_m, \tag{2}$$

$$\mathbf{a}_d = \frac{\mathbf{F}_L + \mathbf{F}_R - B \cdot \mathbf{v}_m}{m}, \tag{3}$$

$$\mathbf{v}_d = \int \mathbf{a}_d dt \tag{4}$$

Equation (1) defines desired acceleration $\mathbf{a}_d$ as proportional to the sum of forces, with virtual mass $m = 3, \mathrm{kg}$, $\mathbf{F}_L$ and $\mathbf{F}_R$ as forces from left and right sensors, and $\mathbf{F}_D$ as resistance force. Equation (2) states $\mathbf{F}_D$ is proportional to velocity $\mathbf{v}_m$ and damping B. Equations (3) and (4) calculate $\mathbf{a}_d$ and desired velocity $\mathbf{v}_d$, respectively. The global coordinate frame is shown in Fig. 1b.

The system includes a virtual environment created in Unity 3D (Unity Technologies), offering real-time visual feedback on task progress. It features automated data processing for efficient handling of sensor measurements, enabling detailed analysis of movement trajectories and force dynamics, allowing this study to investigate bilateral coordination in chronic stroke and healthy individuals.

2.3. Tasks in virtual environment

The task assessed bilateral upper-limb coordination in a virtual environment. While the haptic robot supports 4 DOF, the task was limited to 3 DOF: 2 translational movements in the frontal plane and 1 rotational movement around the sagittal axis. The primary goal was to align a tracking object with a predefined target in the frontal plane (see Fig. 1b). The user was required to use both limbs in coordination, ensuring that the tracking object covered the target object accurately.

The task included 16 sequential targets appearing in a predefined order (see Fig. 3), with movements between consecutive targets. Difficulty was adjusted using damping values of $0\,\frac{\mathrm{N}}{\mathrm{m/s}}$, $20\,\frac{\mathrm{N}}{\mathrm{m/s}}$, and $40\,\frac{\mathrm{N}}{\mathrm{m/s}}$, introducing resistance to user movements.

Visual feedback was implemented in Unity3D, allowing interactivity. The participant's movements were mirrored in the virtual environment, with the tracking object reflecting the bimanual handle's position and orientation in real-time. The target object appeared as a white rectangle, and the tracking object as black (see Fig. 1b). When close to alignment, the tracking object turned yellow. Upon meeting position and orientation criteria (including minimizing undesirable rotations around the X-axis to align with the target orientation of 0°), it turned green, signaling target was properly reached. The system allowed deviations of up to 2 cm in position and 5° in orientation in global frame of the robot. These constraints are visualized in Fig. 3, which includes a global reference frame and markers illustrating the position and orientation margins applied to all targets. Alignment had to be maintained for 3 seconds before the target disappeared and a new one appeared. This process repeated until all 16 targets were covered in three iterations.

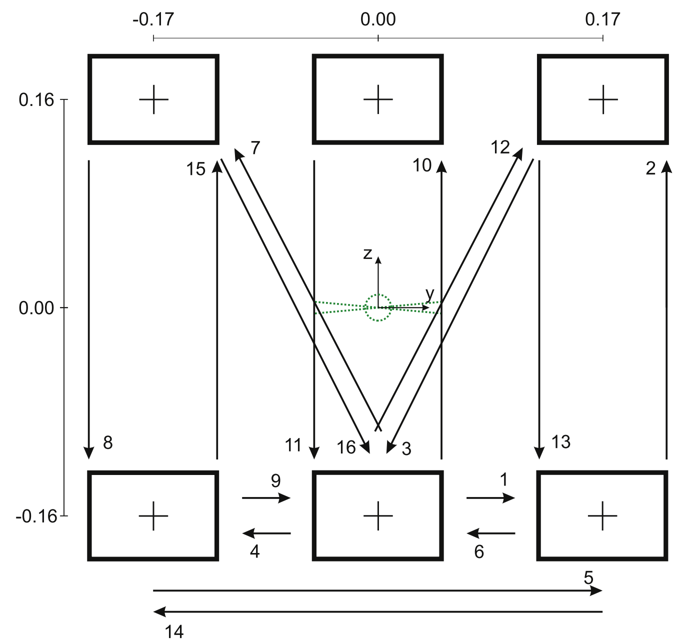

Fig. 3. Target positions and their sequence are indicated by numbered labels. The global coordinate frame is shown along with green dashed markers that illustrate the task constraints: a circle representing the maximum allowed position error, and two lines indicating the orientation error range. These constraints apply to all target locations and are shown at the global origin for reference.

2.4. Measurement protocol

All participants provided informed consent and performed the task standing, including both healthy participants and participants with stroke.

Before starting, participants were briefed on the haptic device and shown its operation. They were positioned in front of a $1.4\,\mathrm{m} \times 1.4\,\mathrm{m}$ screen displaying the virtual environment, with the handle centered along their body's vertical axis. The handle's distance was adjusted so that participants' upper arms remained close to their body in the initial position (see Fig. 1b). Participants were instructed to align the tracking object with the target using coordinated bimanual movements. After a brief demonstration, they performed practice trials to familiarize themselves with the task, receiving feedback and corrections from the supervisor as needed. The practice session lasted about 3 minutes. For participants with impaired grip, a brace was used to secure their hand to the handle, remaining in place throughout the task. Participants were instructed to perform the task calmly and at their own pace, with no time constraints, ensuring they could complete it comfortably. The entire protocol for each participant took approximately 15–20 minutes to complete, though no time limits were imposed.

An essential element of the study was the ability to adjust the level of damping. Damping was introduced in the task through three levels, set at 0 $\frac{\mathrm{N}}{\mathrm{m/s}}$, 20 $\frac{\mathrm{N}}{\mathrm{m/s}}$, and 40 $\frac{\mathrm{N}}{\mathrm{m/s}}$. The protocol included three repetitions per damping level, totaling 48 movements per condition and 144 movements overall. Short breaks were allowed between damping levels.

2.5. Methods for analysis of measurements

During measurements, key signals were recorded to measure participant interactions with the haptic robot, including the end-effector position and forces from both right and left hand sensors. This setup enabled precise monitoring of bimanual coordination and force application. For analysis, trajectories were segmented into movements between targets. Fig. 4a shows segmented trajectories for all participants, both healthy and with chronic stroke. Velocity was derived by differentiating position data, and force signals were similarly segmented, enabling comparative analysis of movement and force patterns between groups.

The manipulation force, which moves the robot, was calculated as the sum of forces from the left and right sensors in the global coordinate frame:

$$\mathbf{F}_{man} = \mathbf{F}_L + \mathbf{F}_R. \tag{5}$$

The internal force, representing forces on the handle that do not contribute to movement [28], was computed as:

$$\mathbf{F}_{int} = \frac{\mathbf{F}_{L,loc} - \mathbf{F}_{R,loc}}{2}, \tag{6}$$

where $\mathbf{F}_{L,loc}$ and $\mathbf{F}_{R,loc}$ are forces in the handle's local coordinate frame. In this frame, the y-axis points from the left to the right sensor, and the z-axis points upward. The local coordinate frame is shown in Fig. 2a.

Forces along the local handle y-axis indicate compressive (positive internal force) or tensile (negative internal force) forces on the handle. Forces along the z-axis cause rotation around the x-axis, requiring correction to align the handle with targets set at 0° rotation, as shown in Fig. 3.

2.5.1. Variability parameters

Fig. 4a shows 16 plots, one per target, displaying trajectories for both healthy participants (blue) and participants with stroke (red). Fig. 4b presents polygon patches enveloping these trajectories. Each patch represents the area containing 90 % of the signal data, excluding the upper and lower 5 % of data points as outliers. Healthy participants' patches are blue, and participants with stroke are red. The area of each polygon patch was calculated, yielding parameter V_T for trajectories. Similar calculations were performed for (a) velocities, resulting in the parameters V_v, (b) manipulation forces, resulting in the parameter V_{FM}, and (c) internal forces, resulting in the parameter V_{FI}. Figs. 5a and 5b show the polygon patches for manipulation force and internal force, respectively.

2.5.2. Direction parameters

Velocity and manipulation force were decomposed into two components. For each target, a unit vector $e_\parallel$ was calculated, pointing from the starting position (initial or previous target) to the current target. A perpendicular unit vector $e_\perp$ (perpendicular to $e_\parallel$) in the YZ plane was also computed. Velocity and manipulation force were projected onto these vectors, yielding: (a) $v_\parallel$ and $F_{M\parallel}$ (parallel to movement direction) and (b) $v_\perp$ and $F_{M\perp}$ (perpendicular to movement direction). Additionally,

Table 1
Table displaying p-values from statistical tests comparing healthy participants and stroke participants across damping levels. Italic numbers indicate p-values between 0.05 and 0.01, and bold numbers indicate p-values below 0.01.

p_{HS}	B0	B20	B40		B0	B20	B40
V_T	0.249	0.367	0.775	V_{FM}	**0.006**	0.561	1.000
V_v	*0.014*	0.270	1.000	V_{FI}	**4.2E-06**	**4.2E-06**	**4.2E-06**
$v_\parallel$	0.058	0.683	0.095	$F_{M\parallel}$	0.086	0.340	0.086
$v_\perp$	0.053	*0.035*	0.104	$F_{M\perp}$	**0.010**	0.065	0.115
$v_{N\perp}$	**7.7E-04**	**0.009**	*0.025*				

Table 2
Table displaying p-values from statistical tests comparing damping levels. Italic numbers indicate p-values between 0.05 and 0.01, and bold numbers indicate p-values below 0.01.

Parameter V_T				Parameter V_{FM}			
	p_{B0B20}	p_{B0B40}	p_{B20B40}		p_{B0B20}	p_{B0B40}	p_{B20B40}
H	0.927	0.683	1.000	H	0.927	**0.007**	0.058
S	0.683	0.425	1.000	S	1.000	0.728	0.249
Parameter V_v				Parameter V_{FI}			
	p_{B0B20}	p_{B0B40}	p_{B20B40}		p_{B0B20}	p_{B0B40}	p_{B20B40}
H	*0.018*	**0.003**	0.775	H	1.000	**0.001**	**0.006**
S	**7.7E-04**	**7.3E-05**	0.292	S	**2.3E-04**	0.292	0.340
Parameter $v_\parallel$				Parameter $F_{M\parallel}$			
	p_{B0B20}	p_{B0B40}	p_{B20B40}		p_{B0B20}	p_{B0B40}	p_{B20B40}
H	0.340	0.425	1.000	H	**4.2E-06**	**4.2E-06**	**7.3E-05**
S	1.000	1.000	0.927	S	**6.1E-06**	**4.2E-06**	**1.3E-05**
Parameter $v_\perp$				Parameter $F_{M\perp}$			
	p_{B0B20}	p_{B0B40}	p_{B20B40}		p_{B0B20}	p_{B0B40}	p_{B20B40}
H	**0.009**	**0.001**	0.683	H	1.000	0.211	0.164
S	**0.008**	**4.9E-04**	0.150	S	0.728	1.000	0.775
Parameter $v_{N\perp}$							
	p_{B0B20}	p_{B0B40}	p_{B20B40}				
H	*0.039*	**0.004**	0.927				
S	**0.005**	**4.2E-04**	0.340				
Parameter F_{IC}				Parameter F_{IR}			
	p_{B0B20}	p_{B0B40}	p_{B20B40}		p_{B0B20}	p_{B0B40}	p_{B20B40}
H	0.367	**1.8E-05**	**0.011**	H	0.395	**0.002**	0.095
S	1.000	1.000	1.000	S	1.000	1.000	1.000

$v_{N\perp}$ was calculated by normalizing $v_\perp$ by $v_\parallel$, representing the normalized perpendicular velocity component. This decomposition allowed detailed analysis of movement dynamics, distinguishing between intended and deviating components.

Internal force was similarly decomposed in the handle's local coordinate frame into: (a) compressive force F_{IC} (along the y-axis) and (b) rotational force F_{IR} (perpendicular to the y-axis, causing handle rotation).

Parameters for each target were aggregated into 16-value vectors, used to generate box plots showing medians and quartiles for healthy and stroke participants. Normality of the data distributions for parameters (V_T, V_v, V_{FM}, V_{FI}, $v_\parallel$, $v_\perp$, $v_{N\perp}$, $F_{M\parallel}$, $F_{M\perp}$, F_{IC}, F_{IR}) was assessed using the Shapiro-Wilk test. Non-normality was observed in a subset of parameters ($p < 0.05$), prompting the use of non-parametric statistical tests to ensure robustness. For between-group comparisons (healthy vs. stroke) in Table 1, the Kruskal-Wallis test was applied to assess differences at each damping level (B0, B20, B40). Bonferroni correction (factor of 3) was used to control the family-wise error rate, with adjusted p-values reported as significant at ($\alpha = 0.05$). For within-group comparisons in Table 2, the Friedman test was used to evaluate differences across damping levels (B0, B20, B40) within each group (healthy

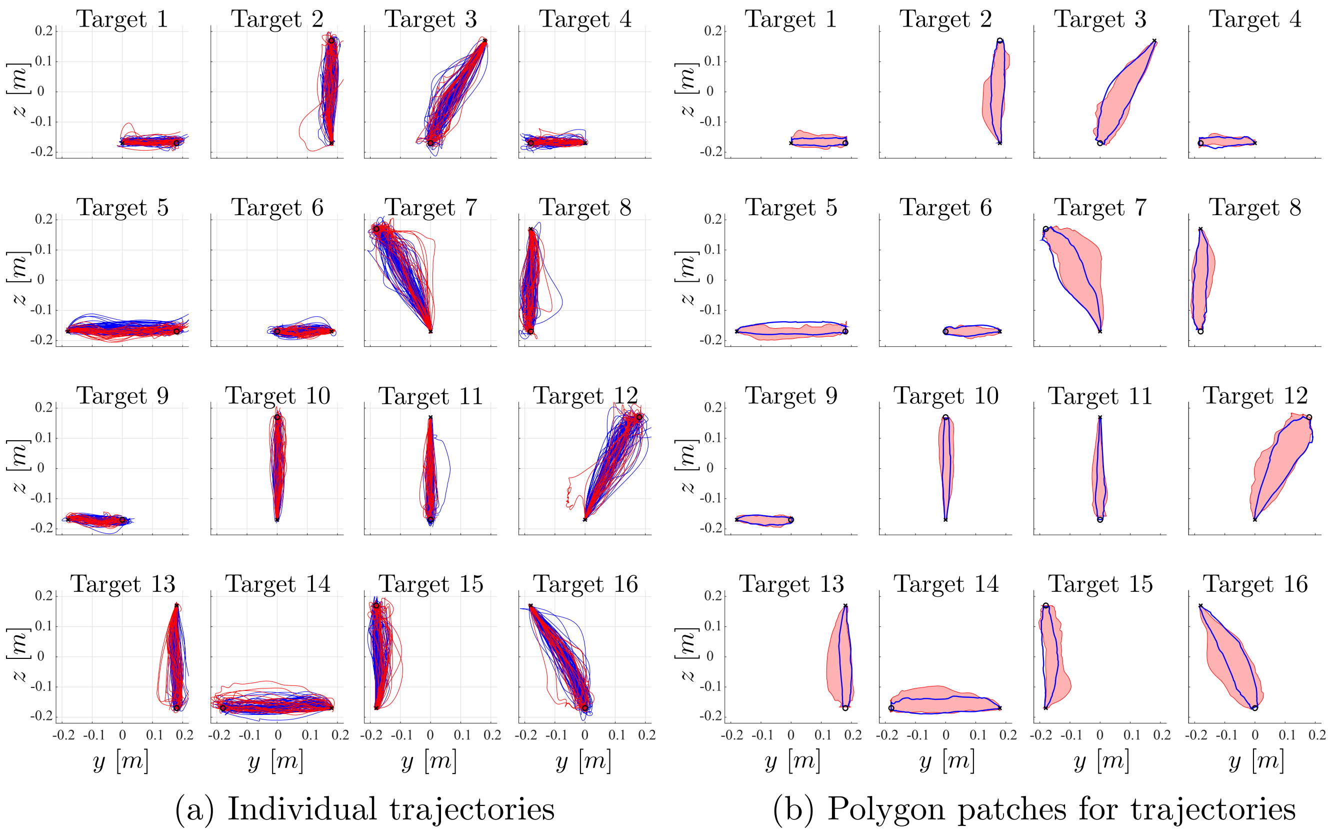

Fig. 4. Trajectories for healthy participants (blue) and stroke participants (red) at 0 Ns/m damping. Subfigure (a) displays trajectories, with circles marking target positions and "x" marks indicating previous targets. Subfigure (b) shows polygon patches for these trajectories.

and stroke). When the Friedman test indicated significant differences ($p < 0.05$), post-hoc Wilcoxon signed-rank tests with Bonferroni correction (factor of 3) were performed for pairwise comparisons (B0 vs. B20, B0 vs. B40, B20 vs. B40), with adjusted p-values significant at ($\alpha = 0.05$). MATLAB analysis code, and data are available at GitHub.[1]

3. Results

This section presents the effects of damping on movement and force dynamics in healthy and chronic stroke participants, analyzed through trajectory, velocity, and force parameters across three damping levels. Fig. 4a shows individual trajectories for each target, with healthy participants in blue and stroke participants in red. Corresponding polygon patches are displayed in Fig. 4b. Figs. 5a and 5b present polygon patches for manipulation and internal forces, respectively. Fig. 6 summarizes variability parameters for trajectories, velocities, manipulation forces, and internal forces across all targets, grouped by damping levels: B0 ($0\,\frac{\mathrm{N}}{\mathrm{m/s}}$), B20 ($20\,\frac{\mathrm{N}}{\mathrm{m/s}}$), and B40 ($40\,\frac{\mathrm{N}}{\mathrm{m/s}}$). The boxplots compare healthy (H) and stroke (S) participants, as well as different damping conditions.

Statistical analysis of V_T, V_v, V_{FM} and V_{FI} parameters between healthy and stroke participants is presented in Table 1. No significant differences were found in V_T at any damping level, indicating trajectory patterns alone cannot distinguish the groups. For velocity, significant differences occurred only at B0, with no differences at B20 or B40, suggesting damping stabilizes movement and reduces group disparities. Similarly, V_{FM} showed significant differences only at B0, mirroring the velocity trend. In contrast, V_{FI} exhibited significant differences across all damping levels, making it the most sensitive parameter for differentiating groups.

Table 2 provides p-values for comparisons between damping levels (B0, B20, B40) within each group. Trajectory parameter V_T showed no significant differences across damping levels for either group, confirming damping has minimal impact on trajectories. For velocity, significant differences were observed between B0 and B20 and B40 but not between B20 and B40, indicating minimal damping reduces velocity variations, with no additional benefit from higher damping. For V_{FM}, healthy participants showed significant differences at B40 compared to B0, suggesting a resistance training effect at medium damping. Stroke participants exhibited no significant differences, though the lowest V_{FM} values occurred at B20 (see Fig. 6), hinting at potential stabilization. For V_{FI}, healthy participants showed significant increases at B40 compared to B0 and B20, supporting a resistance effect. Stroke participants exhibited significant differences between B0 and B20, with B20 minimizing internal forces, potentially stabilizing movements without resistance training.

Figs. 7 and 8 show directional parameters, highlighting group differences and damping effects. Fig. 7 presents velocity parameters: $v_{\parallel}$ (toward the target), $v_{\perp}$ (deviating from the path), and $v_{N\perp}$ (normalized deviation). No significant differences in $v_{\parallel}$ (Table 1) occurred at any damping. For $v_{N\perp}$, significant differences were observed across all damping levels, with stroke participants exhibiting larger deviations (Table 1). While $v_{\parallel}$ values were comparable, higher $v_{\perp}$ and $v_{N\perp}$ values in stroke participants highlighted greater deviations from straight-line movements. When comparing damping levels within groups (Table 2), $v_{\parallel}$ showed no significant differences. For $v_{\perp}$ and $v_{N\perp}$, stroke and healthy participants exhibited decreasing values with higher

[1] https://github.com/janezpodfe/BimanualTaskStrokeStudy

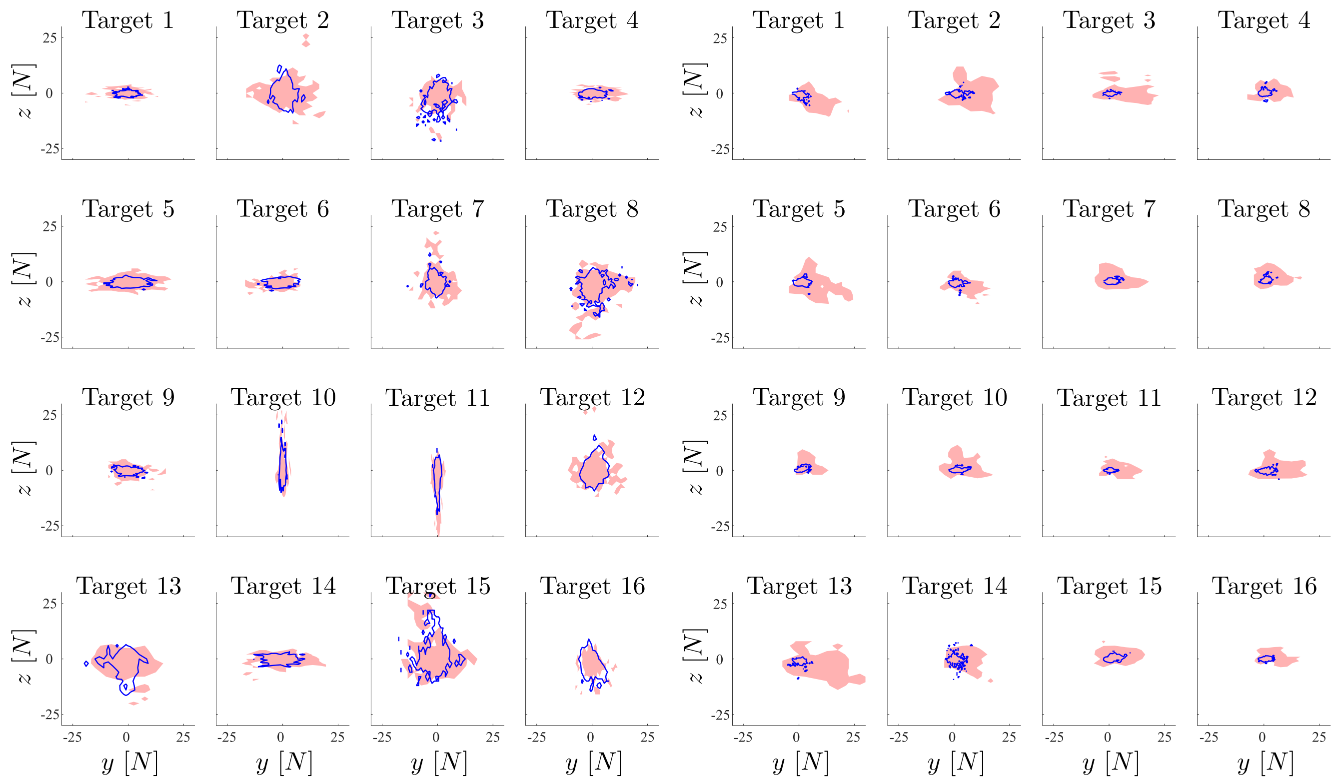

(a) Polygon patches for manipulation force. (b) Polygon patches for internal force.

Fig. 5. Polygon patches for healthy participants (blue) and stroke participants (red) at 0, Ns/m damping. Subfigure (a) shows patches for manipulation forces, and subfigure (b) displays patches for internal forces.

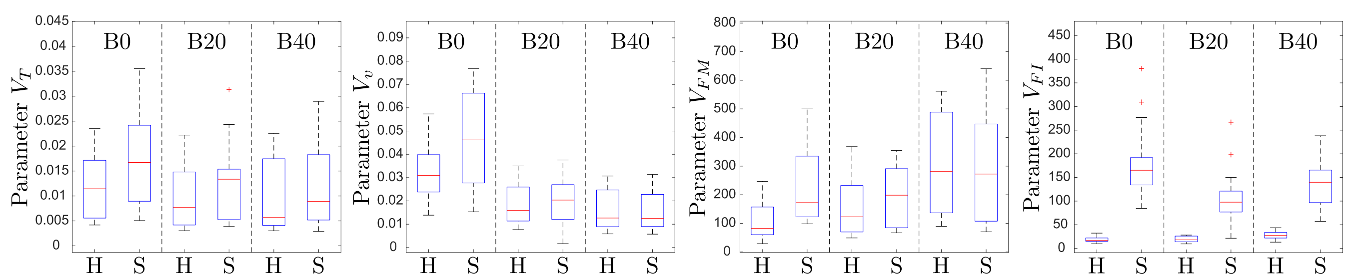

Fig. 6. Boxplots for the parameters V_T, V_v, V_{FM} and V_{FI}. Each boxplot represents the distribution of values collected for movements toward 16 targets. Acronyms denote: H (healthy participants), S (participants with stroke), B0 (damping 0 $\frac{\text{N}}{\text{m/s}}$), B20 (damping 20 $\frac{\text{N}}{\text{m/s}}$), B40 (damping 40 $\frac{\text{N}}{\text{m/s}}$).

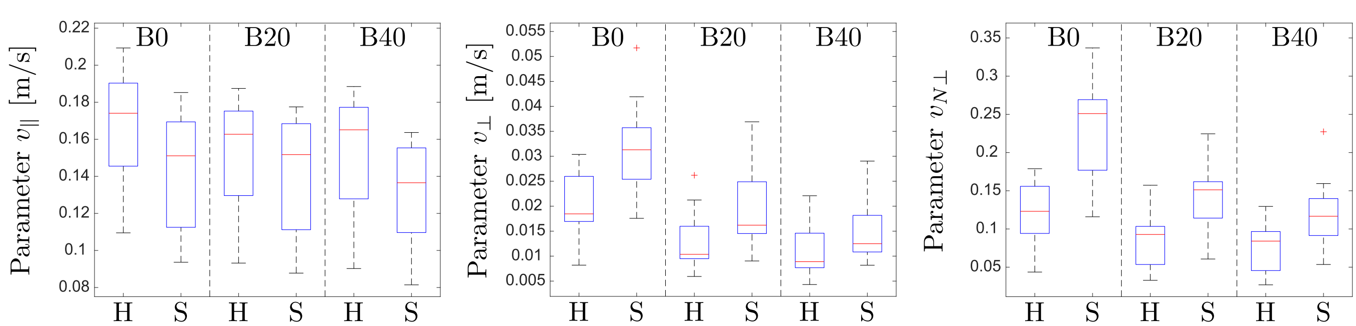

Fig. 7. Boxplots for velocity parameters: $v_{\parallel}$, $v_{\perp}$ and $v_{N\perp}$. Acronyms denote: H (healthy participants), S (participants with stroke), B0 (damping 0 $\frac{\text{N}}{\text{m/s}}$), B20 (damping 20 $\frac{\text{N}}{\text{m/s}}$), B40 (damping 40 $\frac{\text{N}}{\text{m/s}}$).

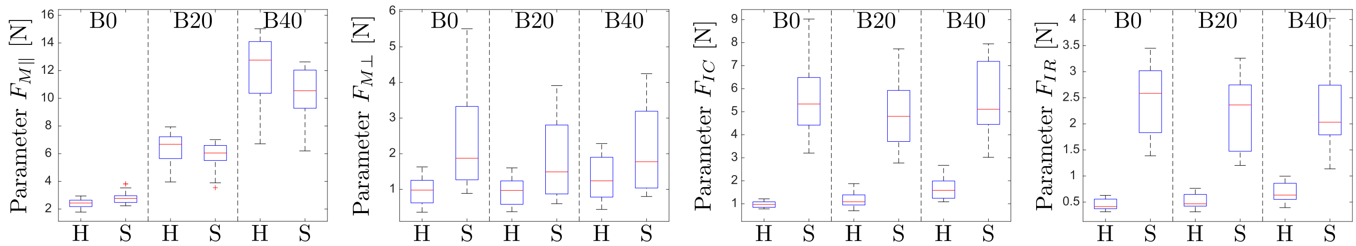

Fig. 8. Boxplots for manipulation and internal force parameters: $F_{M\parallel}$, $F_{M\perp}$, F_{IC} and F_{IR}. Acronyms denote: H (healthy participants), S (participants with stroke), B0 (damping 0 $\frac{\text{N}}{\text{m/s}}$), B20 (damping 20 $\frac{\text{N}}{\text{m/s}}$), B40 (damping 40 $\frac{\text{N}}{\text{m/s}}$).

damping, indicating improved stability. For $v_\perp$ and $v_{N\perp}$ in both groups, significant differences occurred between B0-B20 and B0-B40, with no differences between B20 and B40, suggesting minimal damping effectively reduces deviations.

Fig. 8 illustrates manipulation force parameters: $F_{M\parallel}$ (along the movement path) and $F_{M\perp}$ (deviating from the path). No significant differences in $F_{M\parallel}$ between stroke and healthy participants (Table 1) were observed at any damping level. Significant differences in $F_{M\perp}$ between stroke and healthy participants (Table 1) occurred at B0 but not at B20 and B40, where stroke participants approached healthy levels, indicating damping stabilizes force application. When comparing damping levels (Table 2), $F_{M\parallel}$ showed significant differences across all levels for both groups, reflecting increased effort under higher damping. For $F_{M\perp}$, healthy and stroke participants showed no significant differences, though the lowest values occurred at B20.

Two boxplots on the left side of the Fig. 8 presents internal force parameters: F_{IC} (compressive forces) and F_{IR} (rotational forces). Significant differences between groups occurred across all damping levels (Table 1, $p < .001$), with participants with chronic stroke exhibiting consistently higher internal forces, indicating excessive force application. When comparing damping levels (Table 2), healthy participants showed significant increases in F_{IC} and F_{IR} at B40 compared to B0 and B20, reflecting resistance effects. Stroke participants exhibited no significant differences, though slight decreases in F_{IC} at B20 were observed, suggesting limited damping effects on internal forces.

4. Discussion

This study examined how damping influences bimanual cooperative tasks in healthy and chronic stroke participants, using a haptic robot with dual force sensors to assess movement and force dynamics. The task required explicit interlimb coordination, engaging neural pathways often impaired post-stroke [7,29]. Our system is build upon related concepts as presented in [4], requiring simultaneous limb coordination to engage the beneficial temporal and spatial coupling mechanisms for motor recovery. Adjustable damping and real-time haptic feedback, consistent with the motor learning benefits of robotic training reported by Yang et al. [5], enabled us to investigate the effects of damping on bimanual coordination. Our results show distinct effects of damping on movement and force, revealing group-specific differences. Damping's role in stabilizing task-relevant dimensions (task space) while tolerating variability in task-irrelevant dimensions (null space) aligns with the minimal intervention principle [20]. Notably, trajectory variability remained unaffected across damping levels, indicating that trajectories alone do not distinguish between groups or capture damping effects.

To interpret damping's effects, we draw on motor control theories. The finding that damping has virtually no effect on trajectory shows the robustness of human sensorimotor control, as it demonstrates the ability to prioritize control over task-relevant dimensions, or task space, while allowing flexibility in task-irrelevant dimensions, known as null space. In our task, participants maintained consistent trajectories (task space) despite varying damping, focusing control on target acquisition while tolerating force pattern variability (null space). This behavior is consistent with the minimal intervention principle [20], which posits that the motor system corrects only deviations that interfere with task goals. Similarly, Mistry and Schaal [30] describe how humans achieve precise outcomes by tightly regulating task space variables while exploiting null space flexibility to adapt to perturbations. These findings underscore the efficiency of selective motor control in bimanual tasks and support the design of haptic systems that accommodate natural coordination strategies in stroke rehabilitation.

Damping influenced velocity parameters differently across groups. The parallel velocity ($v_\parallel$) remained stable across damping levels, reflecting self-selected speeds consistent with instructions to perform the task calmly and at their own pace, without time constraints. Higher perpendicular velocities ($v_{N\perp}$) in participants with chronic stroke suggest less direct trajectories, consistent with prior reports of segmented and more variable movements [25,26,29]. Damping significantly reduced deviations, as shown in Table 1 and Table 2 for parameter V_v, improving movement stability in the participants with stroke and aligning their performance more closely with healthy participants. No further improvement was observed at moderate damping (B40), suggesting B20 provides optimal stabilization without the diminishing returns of higher resistance.

Consistent significant differences in $F_{M\parallel}$ across damping levels within both groups reflect the need for increased force to maintain similar velocities under higher damping. Significant differences in the $F_{M\perp}$ parameter between healthy and stroke participants at B0 highlight greater force deviations in stroke participants, which is consistent with their higher trajectory variability and reduced motor control. Damping B20 and B40 reduced perpendicular manipulation force in stroke participants, indicating stabilization effect of damping.

Internal force, reflecting push-pull interactions and undesired handle rotation, was the most sensitive measure for distinguishing groups, with stroke participants showing consistently higher values across all damping levels. This is consistent with prior findings that stroke survivors often rely on inefficient compensatory strategies involving excessive internal forces [18,31,32]. As suggested by analysis of parameter V_{FI}, low damping (B20) minimized internal forces in stroke participants, stabilizing movements without substantial resistance.Moderate damping (B40) compared to no damping (B0) increased internal and manipulation forces in healthy participants, suggesting resistance training effects, but provided no additional stabilization for stroke participants. The analysis of internal force parameters reveals inefficiencies in stroke participants' motor control strategies, with significantly higher internal forces indicating reliance on excessive compensatory patterns during bimanual tasks. These results highlight distinct group responses: B20 modestly stabilizes stroke performance without imposing resistance, while B40 introduces resistance in healthy participants. The persistent internal forces in stroke suggest compensatory patterns are not easily modulated by damping.

Damping affected the two groups differently: B20 improved movement stability in stroke participants without adding resistance, while B40 introduced resistance training effects. These findings emphasize the need to tailor damping to individual therapeutic goals. For stroke rehabilitation, low damping (B20) may optimize stability of movements, while moderate damping (B40) might be useful for strength training in later stages.

Although haptic robot designs often aim to minimize damping [33], our results suggest that low damping can aid stability without shifting into resistance training. Similar benefits have been reported in rowing training with added damping [34]. Recent reviews support resistance training as a promising, though not yet standard, stroke therapy [35]. B40 may reflect such an approach, offering strength gains during advanced rehabilitation. Additionally, even light damping could support individuals with limited tolerance for intensive training [36].

This study's small and unequal sample sizes (13 stroke, 25 healthy participants) limits statistical power and generalizability. The wide age range in the healthy group (23–72 years, mean 36 ± 15) compared to the stroke group (45–83 years, mean 57 ± 11) may introduce confounding effects, as age can influence motor performance [3]. Due to the exploratory nature of this study, age was not controlled for in the statistical analyses, which is a limitation. However, the observed damping effects on movement stabilization in stroke participants are notable and statistically measurable, suggesting the sample was sufficient for detecting key differences. Future larger, balanced studies may provide additional support for these findings by enhancing their generalizability.

5. Conclusion

This study demonstrates the effects of damping on movement and force dynamics in healthy participants and participants with chronic stroke during bimanual tasks, highlighting the need for tailored damping levels to optimize rehabilitation. Low damping (B20) effectively stabilized movements and reduced deviations in stroke participants, resulting in patterns that more closely resembled those of healthy individuals without introducing excessive resistance. This demonstrates the minimal intervention principle, as low damping enhances task-relevant control by stabilizing movements while avoiding overconstraint. Medium damping (B40) acted as resistance training, potentially aiding strength recovery in advanced rehabilitation stages, though its use requires careful evaluation to avoid disrupting coordination.

The findings suggest incorporating low to moderate damping, such as $20\,\frac{\mathrm{N}}{\mathrm{m/s}}$, in haptic robot control design for stroke rehabilitation. This approach stabilizes motor actions and reduces variability, aligning with evidence that low-intensity resistance training enhances recovery in robot-assisted rehabilitation.

CRediT authorship contribution statement

J. Podobnik: Writing – original draft, Visualization, Validation, Software, Methodology, Formal analysis, Data curation; **M. Munih:** Supervision, Resources, Project administration, Funding acquisition, Conceptualization; **M. Mihelj:** Writing – review & editing, Validation, Supervision, Methodology, Formal analysis, Conceptualization.

Declaration of competing interest

As the corresponding author, I declare that there is no conflict of interest related to this work. All authors have approved the final manuscript and agree with its submission.

Acknowledgments

The authors acknowledge the financial support from the Slovenian Research and Innovation Agency (research core funding No. P2-0228).

References

[1] Anwer S, Waris A, Gilani SO, Iqbal J, Shaikh N, Pujari AN, et al. Rehabilitation of upper limb motor impairment in stroke: a narrative review on the prevalence, risk factors, and economic statistics of stroke and state of the art therapies. Healthcare 2022;10(2):190.
[2] Hatem SM, Saussez G, Faille MD, Prist V, Zhang X, Dispa D, et al. Rehabilitation of motor function after stroke: a multiple systematic review focused on techniques to stimulate upper extremity recovery. Front Hum Neurosci 2016;10(3):442–60.
[3] Kilbreath SL, Heard RC. Frequency of hand use in healthy older persons. Austral J Physiother 2005;51(2):119–22.
[4] Rose DK, Winstein CJ. Bimanual training after stroke: are two hands better than one? Top Stroke Rehabil 2004;11(4):20–30.
[5] Yang X, Shi X, Xue X, Deng Z. Efficacy of robot-assisted training on rehabilitation of upper limb function in patients with stroke: a systematic review and meta-analysis. Arch Phys Med Rehabil 2023;104(9):1498–513.
[6] Lee MJ, Lee JH, Koo HM, Lee SM. Effectiveness of bilateral arm training for improving extremity function and activities of daily living performance in hemiplegic patients. J Stroke Cerebrovascular Dis 2017;26(5):1020–5.
[7] Kantak S, Jax S, Wittenberg G. Bimanual coordination: a missing piece of arm rehabilitation after stroke. Restor Neurol Neurosci 2017;35(4):347–64.
[8] La C-SD, Ba, Arias-Montiel M, Lugo-González E. Emg-controlled hand exoskeleton for assisted bilateral rehabilitation. Biocybernetic Biomed Eng 2022;42(2):596–614.
[9] Johnson MJ, Wang S, Bai P, Strachota E, Tchekanov G, Melbye J, et al. Bilateral assessment of functional tasks for robot-assisted therapy applications. Med Biol Eng Comput 2011;49:1157–71.
[10] Mohan DM, Khandoker AH, Wasti SA, Alali S, Jelinek HF, Khalaf K. Assessment methods of post-stroke gait: a scoping review of technology-driven approaches to gait characterization and analysis. Front Neurol 2021;12.
[11] Miao Q, Zhang M, Cao J, Xie S. Reviewing high-level control techniques on robot-assisted upper-limb rehabilitation. Adv Rob 2018;32:1–16.
[12] Trlep M, Mihelj M, Munih M. Skill transfer from symmetric and asymmetric bimanual training using a robotic system to single limb performance. J Neuroeng Rehabil 2012;9:43.
[13] Demir U, Kocaoğlu S, Akdoğan E. Human impedance parameter estimation using artificial neural network for modelling physiotherapist motion. Biocybernetic Biomed Eng 2016;36(2):318–26.
[14] Marchal-Crespo L, Reinkensmeyer DJ. Review of control strategies for robotic movement training after neurologic injury. J Neuroeng Rehabil 2009;6:1–15.
[15] Basteris A, Nijenhuis SM, Stienen A, Buurke JH, Prange GB, Amirabdollahian F. Training modalities in robot-mediated upper limb rehabilitation in stroke: a framework for classification based on a systematic review. J Neuroeng Rehabil 2014;11:1–15.
[16] Liao WW, Wu CY, Hsieh YW, Lin KC, Chang WY. Effects of robot-assisted upper limb rehabilitation on daily function and real-world arm activity in patients with chronic stroke: a randomized controlled trial. Clin Rehabil 2012;26(2):111–20.
[17] Sy J, Shin KM, J H. Resistive versus active assisted robotic training for the upper limb after a stroke: a randomized controlled study. Ann Phys Rehabil Med 2024;67(1):101789.
[18] Noohi E, Žefran M. Estimating human intention during a human-robot cooperative task based on the internal force model. In: Trends in control and decision-Making for human-Robot collaboration systems. Cham; Springer International Publishing; 2017, p. 83–109.
[19] Tanaka Y, Goto R. A robotic rehabilitation system for cooperative motor training: a preliminary study in a balance seesaw task. In: 2018 IEEE International conference on cyborg and bionic systems (CBS). 2018, p. 216–21.
[20] Todorov E, Jordan MI. Optimal feedback control as a theory of motor coordination. Nat Neurosci 2002;5(11):1226–35.
[21] Nassar A, Vérité F, Pechereau F, Morel G, Vitrani MA. Adaptative damping assistance in bimanual laparoscopic surgery. Int J Comput Assist Radiol Surg 2023;18(4):741–51.
[22] Küçüktabak EB, Kim SJ, Lynch WY, Pons K, J L. Human-machine-human interaction in motor control and rehabilitation: a review. J Neuroeng Rehabil 2021;18:1–18.
[23] Basteris A, Nijenhuis S, Stienen A, Buurke J, Prange G, Amirabdollahian F. Training modalities in robot-mediated upper limb rehabilitation in stroke: a framework for classification based on a systematic review. J Neuroeng Rehabil 2014;11:111.
[24] Munih M, Mihelj M. Psychophysiological responses during robot-assisted rehabilitation. Academic Press; 2018.
[25] Cirstea MC, Levin MF. Compensatory strategies for reaching in stroke. Brain 2000;123(5):940–53.
[26] Levin MF. Interjoint coordination during pointing movements is disrupted in spastic hemiparesis. Brain 1996;119(1):281–93.
[27] Linde RQ, Lammertse P. Hapticmaster - a generic force controlled robot for human interaction. Industrial Robot: An International Journal 2003;30(6):515–24.
[28] Zefran M. Continuous methods for motion planning. Tech. Rep.; University of Pennsylvania; 1996.
[29] Lewis GN, Byblow WD. Bimanual coordination dynamics in poststroke hemiparetics. J Mot Behav 2004;36(2):174–88.
[30] Mistry M, Schaal S. Representation and control of the task space in humans and humanoid robots. CRC Press/Taylor & Francis; 2015, p. 129–50.
[31] Santis D, Mireles D, Squeri E, Morasso V, Zenzeri P, J. Dealing with instability in bimanual and collaborative tasks. In: Proc. 2015 37th annual international conference of the IEEE engineering in medicine and biology society (EMBC). 2015 37th Annual International Conference of the IEEE Engineering in Medicine and Biology Society (EMBC); 2015, p. 1417–20.
[32] Potts CA, Kantak SS. Post-stroke deficits in the anticipatory control and bimanual coordination during naturalistic cooperative bimanual action. J Neuroeng Rehabil 2023;20(1):153.

[33] Leconte P, Stoquart G, Lejeune T, Ronsse R. Rhythmic robotic training enhances motor skills of both rhythmic and discrete upper-limb movements after stroke: a longitudinal pilot study. Int J Rehabil Res 2018;42:1.

[34] Rauter G, Sigrist R, Riener R, Wolf P. Learning of temporal and spatial movement aspects: a comparison of four types of haptic control and concurrent visual feedback. IEEE Trans Haptics 2015;8(4):421–33.

[35] Veldema J, Jansen P. Resistance training in stroke rehabilitation: systematic review and meta-analysis. Clin Rehabil 2020;34:1173–97.

[36] Coroian F, Jourdan C, Bakhti K, Palayer C, Jaussent A, Picot MC, et al. Upper limb isokinetic strengthening versus passive mobilization in patients with chronic stroke: a randomized controlled trial. Arch Phys Med Rehabil 2017;99.